PROCEEDINGS of the
23rd International Congress on Acoustics
9 to 13 September 2019 in Aachen, Germany

Off-line envelope estimation for acoustic screens with uncertain properties

Mathieu GABORIT[(1,2)], Olivier DAZEL[(1)], Peter GÖRANSSON[(2)]

[(1)]LAUM UMR CNRS 6613, Le Mans Université, Le Mans, France
[(2)]MWL, KTH Royal Institute of Technology, Stockholm, Sweden

Abstract

The development of new solutions to reduce impact of noise receives constant attention both from the research and engineering communities. Even though the proposed systems tend to diversify, multi-layered absorbers based on foams remain the most common. Such structures feature one or several thick slabs of foam and are completed by protective or tuning layers of small thickness inserted between slabs or on the free surface. These layers (acoustics screens or films) bring a number of challenges. Firstly, their thickness makes them hard to characterise and some parameters are uncertain. Secondly, the bonding to the surrounding system alter the effective properties. Given the strong influence the films have on the system's response, it appears important to account for these uncertainties from the design phase on. The present contribution introduces a new technique to efficiently account for uncertainty linked to the screens. More precisely, the proposed approach is based on separating the average film influence from the deviation due to uncertainties. This allows to estimate the response envelope using a pre-computed average response and the properties. The results computed for a range of typical and challenging configurations are promising and validate the robustness of the method at any angle of incidence.

Keywords: poroelastic media, uncertainties, envelope curves

1 INTRODUCTION

The requirements in terms of noise reduction keep being raised so to reduce the impact on health and wellness [1, 2]. This trend calls for a better understanding of the most common noise absorbers and for new ways way towards optimised systems. The context of the present study is composite absorbers usually constructed by assembling several layers of poroelastic media [3]. This is a widely used strategy to create absorbing panel and it proved to be efficient on a wide frequency band at a reasonable cost. Many contributions from the literature study this kind of absorbers [3, 4] or their modelling [5, 6, 7] and thus, for conciseness, this part will not be considered in the following.

The films often added on the absorber's free surface are one of the easiest ways to to tune these absorbers [8]. Despite their usual thinness (sub-millimetre), these components alter the coupling between the surrounding air and the absorbing layers and tend to improve the performances if chosen carefully. Nevertheless, their nature and geometry imply a difficult characterisation [9, 10] and thus, reported values for the different parameters of these media are often inaccurate. In the present contribution, the choice is made to account for these uncertainties and represent the systems' response as an envelope controlled by the film's most uncertain parameters.

The remainder of this contribution is as follows. After this introduction, a second section briefly presents how to separate the contribution of the uncertainties that apply to one of the parameters and to derive its influence on the classical quantities of interest. It is shown how these developments allow to quickly generate envelopes around an average response so to represent the system's variability. A third section gathers examples of using the method both for simulating a response and for annotating an envelope on measured responses. A last section discusses the results and concludes.

In the following, a positive time convention $e^{j\omega t}$ is used where $j = \sqrt{-1}$ is the imaginary number, t the time variable and ω the angular frequency.

2 Theory

This first part studies systems such as the one shown in figure Figure 1 and their responses to an excitation by a PW. Particularly, the aim is to identify how the uncertainty on one of the film's parameters impacts the overall behaviour.

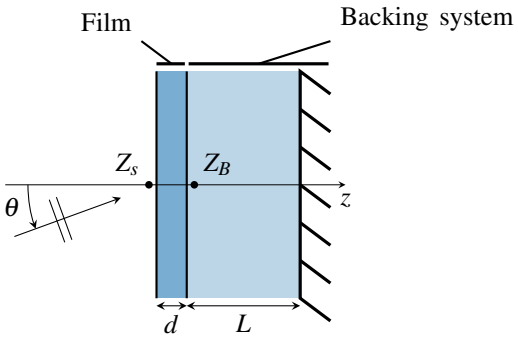

Figure 1. Model under study. A laminate which surface layer is a thin film ($d \ll 1$) is impinged by an air-borne wave. Despite the backing system being represented as a single layer on a rigid backing, the proposed approach can handle more intricate backings without requiring adaptation.

The film is thin ($d \ll 1$) and it is proposed to neglect the elastic effects, focusing mostly on the impact on air-borne waves and considering the film as an equivalent fluid [3]. Regarding the mathematical modelling, this assumption allows to represent the film through an equivalent density ρ_f and compressibility K_f which in turn can be combined to access the associated characteristic impedance Z_f and the wavenumber k_f:

$$Z_f = \sqrt{\rho_f K_f}, \qquad k_f = \omega \cos\theta \sqrt{\frac{\rho_f}{K_f}} \tag{1}$$

where θ is the incidence angle of the wave impinging the laminate.

A key point of the development is to identify that one can derive the surface impedance Z_s for any backing impedance Z_B through the knowledge of the film's properties and geometry. Indeed the impedance translation theorem yields

$$Z_s = Z_f \frac{Z_B + \mathrm{j} Z_f \tan k_f d}{Z_f + \mathrm{j} Z_B \tan k_f d}. \tag{2}$$

Assuming the film is thin with respect to the wavelength such that $k_f d \ll 1$, it comes that the tangents in (2) can safely be approximated by their first order Taylor expansion which, after simplification, leads to

$$Z_s \approx \frac{Z_B + \mathrm{j} Z_f k_f d}{1 + \mathrm{j} Z_B Z_f^{-1} k_f d}. \tag{3}$$

In order to further simplify the expression, a stronger assumption must be considered. In cases where $Z_B \simeq Z_f$ (which turns out to be true in many cases due to the highly resistive nature of the films [3, 11]) the denominator can be approximated by a second Taylor expansion ($(1+\varepsilon)^{-1} = 1 - \varepsilon + \mathcal{O}(\varepsilon^2)$ with $\varepsilon \ll 1$).

Substituting in (3), distributing the product, replacing Z_f and k_f by their expressions from (1) and neglecting the second order terms yields

$$Z_s = Z_B - \mathrm{j}\omega d \cos\theta Z_B^2 K_f^{-1} + \mathrm{j}\omega d \cos\theta \rho_f. \tag{4}$$

This expression describes the surface impedance of systems where a thin, resistive film is placed atop a so-called backing system represented through its acoustic impedance Z_B in cases where the film is considered as an equivalent fluid.

In the context of this contribution, one of the film's parameters is imprecisely known which in turns affect the different geometrical and physical descriptors K_f, ρ_f and d. Mathematically, the uncertainty is accounted for by representing each descriptor ξ by the sum of a *nominal* value $\bar{\xi}$ and the associated deviation $\Delta\xi$. In the remainder of this paper, only uncertainties on parameters ρ_f alone are discussed. Extending the approach to other parameters and descriptors is straightforward. As a last note, the equivalent fluid model used in the present document is a motionless skeleton model commonly known as the Johnson-Champoux-Allard (JCA) model [12, 13, 3]. In the scope of said model, a modification of ρ_f alone occurs if the airflow resistivity σ is uncertain.

Replacing $\rho_f = \bar{\rho}_f + \Delta\rho_f$ into 4 leads to

$$Z_s = \overbrace{Z_B\left(1 - \mathrm{j}\omega d\cos\theta Z_B K_f^{-1}\right) + \mathrm{j}\omega d\cos\theta\bar{\rho}_f}^{\bar{Z}_s} + \underbrace{\mathrm{j}\omega d\cos\theta\Delta\rho_f}_{\Delta Z_s}. \tag{5}$$

where the first part $\bar{Z}_s$ is entirely determined from the nominal value of ρ_f and other deterministic quantities (such as the backing impedance Z_B) and the second ΔZ_s is directly linked to the uncertainties.

From the overall surface impedance Z_s and the surrounding air characteristic impedance Z_0, it is straightforward to derive the reflection coefficient R in a purely deterministic case:

$$R = \frac{Z_s - Z_0}{Z_s + Z_0}. \tag{6}$$

Then, to obtain the so-called nominal and deviated components $\bar{R}$ and ΔR, (5) is substituted into (6). Factorizing $\bar{Z}_s + Z_0$ at the numerator and denominator, the latter takes the form of $1+\varepsilon$ with the small parameter being $\Delta Z_s(\bar{Z}_s + Z_0)^{-1}$. This last operation allows to use once more a first order Taylor expansion such that

$$R = \underbrace{\frac{\bar{Z}_s - Z_0}{\bar{Z}_s + Z_0}}_{\bar{R}}\left(1 + \underbrace{\frac{2Z_0\Delta Z_s}{\bar{Z}_s^2 - Z_0^2}}_{\eta}\right) + \mathcal{O}\left(\frac{\Delta Z_s^2}{\bar{Z}_s^2 - Z_0^2}\right) \tag{7}$$

Equation (7) introduces the parameter η which turns out to control both the deviation of R and of the absorption coefficient $\alpha = 1 - |R|^2 = 1 - |\bar{R}|^2|1+\eta|^2$. To further detail the expression it is important to note that η is complex (due to both its denominator and numerator being complex) and formally writes $\eta = \eta' + \mathrm{j}\eta''$, which after substitution into the expression of α and simplification leads to:

$$\alpha = \underbrace{1 - |\bar{R}|^2}_{\bar{\alpha}} + \underbrace{|\bar{R}|^2\left(2\eta' + |\eta|^2\right)}_{\Delta\alpha} \tag{8}$$

From equations (7) and (8), it is clear that evaluating η for all frequencies allows to compute the deviation of α and hence generate an envelope from an average response. This process, hereby called *envelope annotation*, is completely independent of the determination of the average response itself. Note that in the case of uncertainties impacting the other descriptors (d for instance) if might be needed to computed the average backing surface impedance Z_B using the translation theorem. Indeed, introducing $d = \bar{d} + \Delta d$ in (4) shows that Z_B appears in the computation of η.

Table 1. Properties of media used in tests, the ones for simulations are taken from the literature [14]. CL stands for characteristic length and only the Johnson-Champoux-Allard parameters are available for the second experimental media.

	Simulations		**Experiments**	
Property [unit]	Foam	Film	Foam	Film
Open-Porosity ϕ	0.994	0.99	0.97	0.07±0.01
Airflow resistivity σ [N·s·m^{-4}]	9045	$65{\cdot}10^3$	$23{\cdot}10^3$	$(1120.2{\pm}161.6){\cdot}10^{-3}$
Dynamic Tortuosity α_∞	1.02	1.98	1.06	1.14
Thermal CL Λ' [μm]	197	120	149	42±1
Viscous CL Λ [μm]	103	37	54	42±1
Density ρ_1 [kg·m^{-3}]	8.43	16		
Poisson ratio ν	0.42	0.3		
Young's modulus E [Pa]	$194.9{\cdot}10^3$	$46.8{\cdot}10^6$		
Loss factor	0.05	0.1		

3 APPLICATIONS

In order to demonstrate the technique, two examples are provided in this section. The first one uses the proposed approach to generate envelope curves from scratch and compare the results with the results of Monte Carlo simulations. The second, uses actual measurements of a two-layers system's response to compute an average reponse and annotate an envelope using the films parameters.

In both cases, the system considered is similar to the one in Figure 1. The dimensions used are $d = 0.5$ mm and $L = 20$ mm for the first test case and $d = 0.3$ mm and $L = 17.2 \pm 0.3$ mm for the second (the uncertainty on L is linked to small differences in the porous backing samples geometry). The films and backing media properties for both cases are presented in Table 1. The properties of air are as follows: $\rho_0 = 1.213$ kg·m^{-3}, $\mathrm{Pr} = 0.71$, $\eta_0 = 1.839 \cdot 10^{-5}$ Pa·s, $P_0 = 1.01325 \cdot 10^5$ Pa and $\gamma_0 = 1.4$.

In order to render the results analysis easier, not only the absorption coefficient of the laminates is presented but also the so-called *centred envelope* for which the nominal response is subtracted to all plotted quantities. Note that the nominal response is the one obtained when all the parameters have their nominal value and that, because of the inherent non-linearity of the models and sampling concerns, this response might be different from the actual *average* one.

3.1 Computing a response envelope

In the first test case, the envelopes generated by the proposed method are compared to Monte Carlo simulations with a set of 300 samples drawn from a normal deviation. On this basis, a so-called observed envelope is computed by adding (or subtracting) the sample-wise standard deviation to the sample-wise average. These quantities are computed both at normal incidence $\theta = 0$ rad and at $\theta = \frac{\pi}{3}$ rad and shown respectively in Figures 2 and 3. The Monte Carlo results are generated using a in-house solver [15] that implements a method from the literature [7]. For this test, the backing PEM is modelled as a Biot-JCA material (hence including mechanical effects) and the film as a limp medium [3, 16, 17].

The empirical envelopes are computed from the Monte Carlo simulations by adding (or subtracting) the sample-wise deviation to the sample-wise average. For both figures, these envelopes are closely following these computed using the proposed approach and a deviation of 1β (with β the standard deviation of the uncertain parameter, set to 20% of the nominal value here). The method gives reliable results both at normal incidence (Figure 2) and at oblique incidence (Figure 3).

It is observed that the 1β curves fits correctly the empirical standard deviation envelope, which is an expected

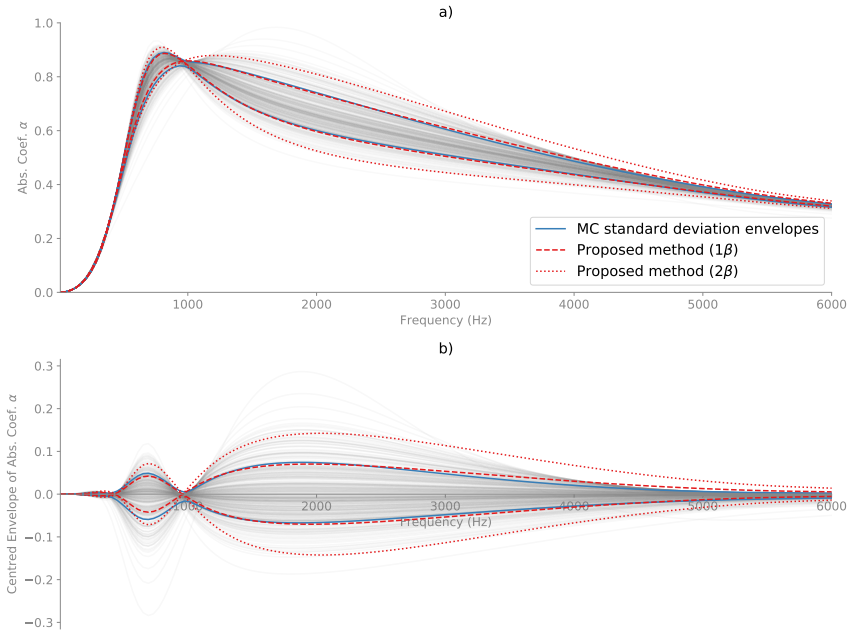

Figure 2. Comparison of the Monte Carlo envelopes (solid line) and the results of the proposed approach (dashed line for one standard deviation of the uncertain parameter and dotted line for two) at normal incidence. Light lines are Monte Carlo realisations. a) Absorption coefficient. b) Centred envelope.

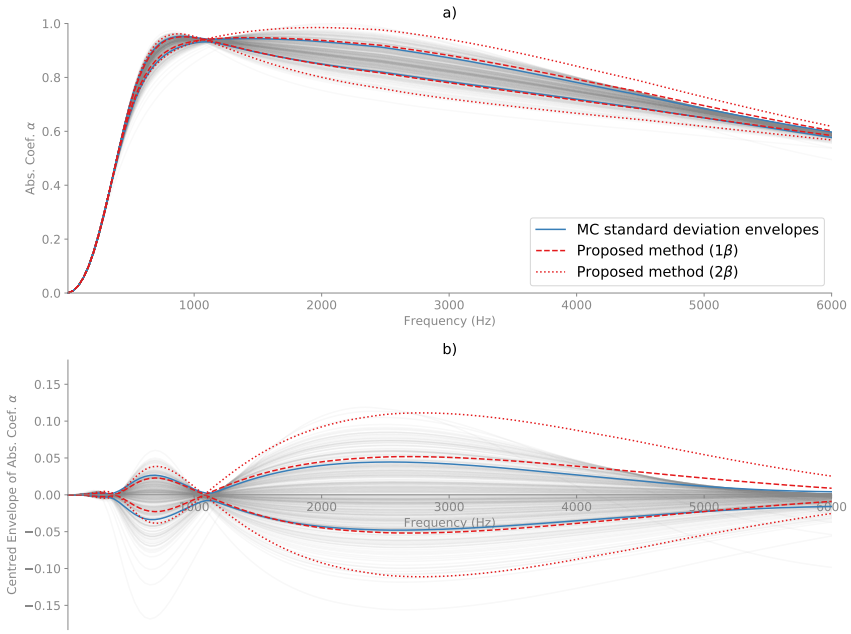

Figure 3. Comparison of the Monte Carlo envelopes (solid line) and the results of the proposed approach (dashed line for one standard deviation of the uncertain parameter and dotted line for two) at $\theta = \pi/3$ rad. Light lines are Monte Carlo realisations. a) Absorption coefficient. b) Centred envelope.

result. Note though that a number of realisations remain out of the envelope. The uncertain parameter (σ in the present case) is drawn from a normal law, centred on its nominal value. Then, the 1β envelope then correspond to the 95% confidence interval and one could reach higher confidence values by computing the envelopes for 2β (as presented on the figures) or even 3β.

Similar tests were performed for other media and backing structures, leading to similar results, not reported here for conciseness. Note that the tests are not performed at high frequency and that the film parameters ensure that none of the assumptions are violated. A more thorough testing is require to fully validate the approach

3.2 Envelope annotation on experimental results

In the second test, three experimental measurements of the absorption coefficient of three samples of a multi-layer system are used as an input. Using these, an average response is computed and an envelope annotated from the statistical characterisation of the film. The parameters are recalled in Table 1 and from the associated uncertainties, the envelope is generated for a variation of the airflow resistivity σ. Note that some discrepancies are expected as only 3 traces of the full system and of the films are released (which clearly is not enough for statistical meaningfulness).

As seen in the previous test, envelopes generated for 1β tend to let many traces out of the envelope. In this second test and, which results are presented on Figure 4, the envelopes are generated for deviations of both 1β and 2β.

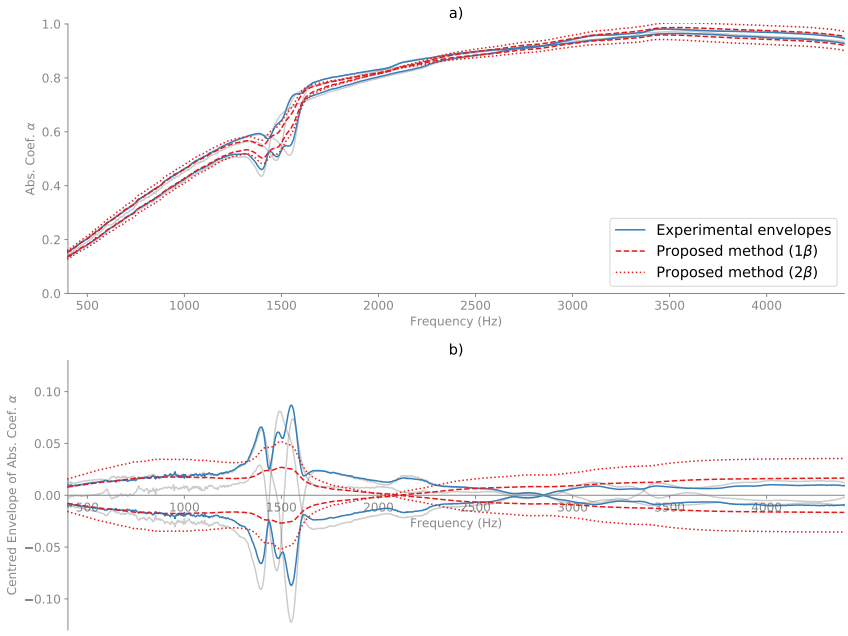

Figure 4. Comparison between the envelopes annotated on experimental results (dotted and dashed lines), experimental traces (light lines) and empirical envelope (solid lines, average plus/minus standard deviation) under normal incidence. a) Absorption coefficient. b) Centred envelope.

Several phenomena are seen on the figure. First, it is observed that, as for simulations, the 1β envelope fit reasonably well the empirical envelope except around the resonances observed at 1500 Hz. The said resonance being due to mechanical effects which are not accounted for in the equivalent fluid model used both for the foam and film, it is not accurately represented in the envelope. Note though that, despite not formally accounting for mechanical effects in the film, the annotation is based on the experimental traces and thus partly

accounts for the resonance. On this side, using 2β as a deviation allows to better fit with the experimental envelopes, as seen on Figure 4. This last remark illustrate the fact the the datasets are very scarce which makes all statistical usage quite subject to deviation.

4 CONCLUSIONS

The method proposed in this contribution is a fast solution for generating envelope curves straight from the parameters of the considered system or over experimental data. This so-called *envelope annotation* process is fast and requires only little information about the system. The developments come at the cost of using a equivalent fluid model for film placed upstream. This implies little to no information about mechanical effect will be rendered. Extending the method this way would be of great interest.

ACKNOWLEDGEMENTS

The authors thank the Matelys Research Lab and particularly L. Jaouen for the support and providing the experimental traces used in section

REFERENCES

[1] M. E. Beutel, C. Jünger, E. M. Klein, P. Wild, K. Lackner, M. Blettner, H. Binder, M. Michal, J. Wiltink, E. Brähler, and T. Münzel. Noise Annoyance Is Associated with Depression and Anxiety in the General Population- The Contribution of Aircraft Noise. *PLOS ONE*, 11(5):e0155357, May 19, 2016. M. A. Andrade-Navarro, editor. DOI: 10.1371/journal.pone.0155357.

[2] World Health Organisation. *Burden of Disease from Environmental Noise: Quantification of Healthy Life Years Lost in Europe*. F. Theakston, editor. World Health Organization Europe, Copenhagen, Denmark, 2011. 106 pages. OCLC: 779684347.

[3] J.-F. Allard and N. Atalla. *Propagation of Sound in Porous Media: Modelling Sound Absorbing Materials*. Wiley, Hoboken, N.J, 2nd edition, 2009. 358 pages.

[4] B. Brouard. *Validation Par Holographie Acoustique de Nouveaux Modèles Pour La Propagation Des Ondes Dans Les Matériaux Poreux Stratifiés*, 1994.

[5] Q. Serra, M. N. Ichchou, and J.-F. Deü. On the Use of Transfer Approaches to Predict the Vibroacoustic Response of Poroelastic Media. *Journal of Computational Acoustics*, 24(02):1550020, June 2016. DOI: 10.1142/S0218396X15500204.

[6] J. P. Parra Martinez, O. Dazel, P. Göransson, and J. Cuenca. Acoustic analysis of anisotropic poroelastic multilayered systems. *Journal of Applied Physics*, 119(8):084907, Feb. 28, 2016. DOI: 10.1063/1.4942443.

[7] O. Dazel, J.-P. Groby, B. Brouard, and C. Potel. A stable method to model the acoustic response of multilayered structures. *Journal of Applied Physics*, 113(8):083506, 2013. DOI: 10.1063/1.4790629.

[8] F. Chevillotte. Controlling sound absorption by an upstream resistive layer. *Applied Acoustics*, 73(1):56–60, Jan. 2012. DOI: 10.1016/j.apacoust.2011.07.005.

[9] ISO. ISO 9053-1 - Acoustics - Determination of airflow resistance - Static airflow method, 2018.

[10] L. Jaouen and F.-X. Bécot. Acoustical characterization of perforated facings. *The Journal of the Acoustical Society of America*, 129(3):1400–1406, 2011. DOI: 10.1121/1.3552887.

[11] N. Atalla and F. Sgard. Modeling of perforated plates and screens using rigid frame porous models. *Journal of Sound and Vibration*, 303(1-2):195–208, June 2007. DOI: 10.1016/j.jsv.2007.01.012.

[12] D. L. Johnson, J. Koplik, and R. Dashen. Theory of dynamic permeability and tortuosity in fluid-saturated porous media. *Journal of fluid mechanics*, 176(1):379–402, 1987.

[13] Y. Champoux and J.-F. Allard. Dynamic tortuosity and bulk modulus in air-saturated porous media. *Journal of Applied Physics*, 70(4):1975, 1991. DOI: 10.1063/1.349482.

[14] M. Gaborit, O. Dazel, and P. Göransson. A simplified model for thin acoustic screens. *The Journal of the Acoustical Society of America*, 144(1):EL76–EL81, July 2018. DOI: 10.1121/1.5047929.

[15] M. Gaborit and O. Dazel. Pymls: Multilayer Solver in Python for acoustic problems, Feb. 2019. DOI: 10.5281/zenodo.2558137.

[16] M. A. Biot. Theory of Propagation of Elastic Waves in a Fluid-Saturated Porous Solid. *The Journal of the Acoustical Society of America*, 28(2):168, 1956. DOI: 10.1121/1.1908239.

[17] O. Dazel, B. Brouard, C. Depollier, and S. Griffiths. An alternative Biot's displacement formulation for porous materials. *The Journal of the Acoustical Society of America*, 121(6):3509, 2007. DOI: 10.1121/1.2734482.